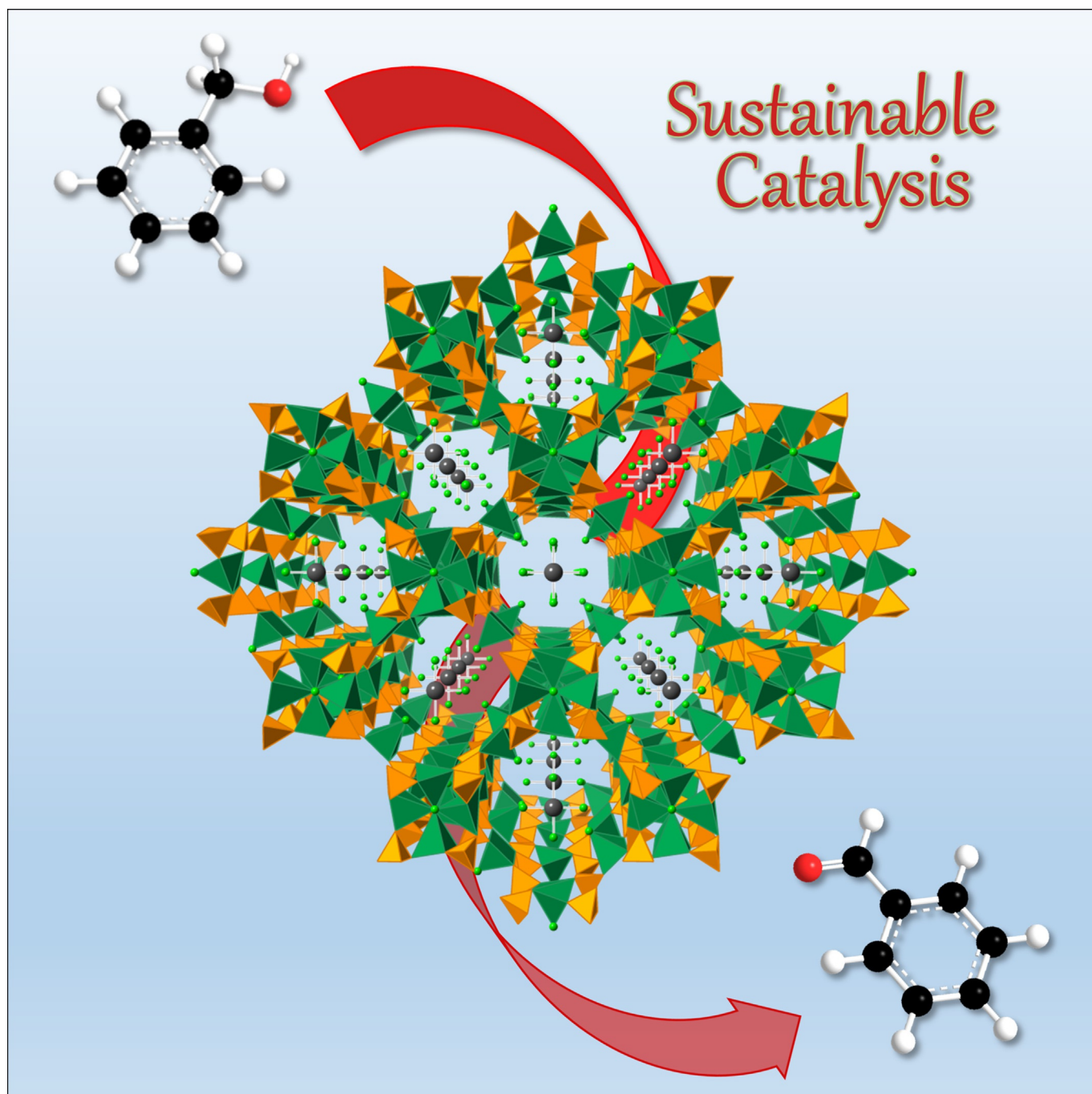


Utilizing Benign Oxidants for Selective Aerobic Oxidations Using Heterogenized Platinum Nanoparticle Catalysts

Christopher S. Hinde,^[a] Arran M. Gill,^[a] Peter P. Wells,^[b, c] T. S. Andy Hor,^[d, e] and Robert Raja^{*[a]}



By using platinum nanoparticle catalysts that are generated in situ by extrusion from a porous copper chlorophosphate framework, the role of oxidants in the selective oxidation of benzyl alcohol to benzaldehyde was evaluated, with a view to establishing structure–property relationships. With a detailed study of the kinetic properties of the oxidation reaction, it has been determined that the aerobic oxidation pathways progress with lower levels of product selectivity and higher activation energies (72.4 kJ mol^{-1}) than the peroxide-based ones (23.6 kJ mol^{-1}); affording valuable insights in the design of solid catalysts for selective oxidation reactions. Furthermore, through the use of X-ray absorption spectroscopy, the effect of calcination temperature on the degree of extrusion and its influence on nanoparticle formation have been evaluated, leading to the establishment of structure–activity correlations between the observed activation energies and the proportion of nanoparticle species generated.

Oxidation reactions are ubiquitous in the pharmaceutical and fine-chemical industries, and are fundamentally important for introducing oxygen-rich functional groups to organic molecules. For example, aldehyde- and ester-containing molecules are heavily employed as flavouring and fragrance agents owing to their volatility and distinctly aromatic nature they are often pleasing to smell and taste.^[1] Benzaldehyde is a key component for most almond-based flavourings, although it finds other uses as a precursor for plastic additives and as an intermediate in the synthesis of antibiotic drugs such as chloramphenicol and ampicillin, as well as stimulants like ephedrine.^[2] Industrially, it is synthesized by the hydrolysis of benzal chloride; however, the dehydrogenative oxidation of benzyl alcohol is a viable, chloride-free and environmentally benign alternative.^[2]

Traditionally, industrial oxidation reactions are based on the use of stoichiometric quantities of inorganic metal-based oxi-

dizing agents such as MnO_2 and CrO_3 , or harsh mineral acids like H_2SO_4 and HNO_3 , which result in hazardous, corrosive and toxic operating conditions as well as the generation of large quantities of polluting waste by-products.^[3] Due to the heightened demand for the chemical and related industries to reduce their negative impact on the environment, there is a significant drive to find alternative economic and sustainable oxidation reagents and synthetic protocols.^[3] The abundance of molecular oxygen, its high atom-economy in oxidation reactions, low cost and mild reaction conditions make it an appealing candidate as an oxidant,^[4] although high-pressure and relatively high reaction temperatures are often required, since the reaction occurs in the gas phase. Similarly, simple peroxides such as H_2O_2 and *tert*-butyl hydroperoxide (TBHP) are often considered as alternative green oxidants.^[4] Although, their use often leads to the generation of larger quantities of by-products in comparison to reactions with molecular oxygen, these oxidants are slightly more reactive due to the lower bond dissociation energy (BDE) of the single O–O bond ($49.7 \text{ kcal mol}^{-1}$ for H_2O_2 and $45.0 \text{ kcal mol}^{-1}$ for TBHP)^[5] relative to the O=O bond ($118 \text{ kcal mol}^{-1}$),^[6] with the added potential to operate under comparatively mild conditions. Nonetheless, suitable catalysts are often still required to activate the oxidants in order to achieve satisfactory activity and selectivity within reasonable reaction conditions.

In recent years, supported noble-metal nanoparticle (NP) catalysts have shown great promise in the activation of both molecular oxygen^[7] and simple peroxides^[8] for the selective oxidation of alcohols, and more recently, the activation of C–H bonds in hydrocarbon substrates such as toluene.^[8c,9] We recently reported a new method for the synthesis of highly active, uniform and site-isolated metal NPs in situ, by extrusion of chlorometalate precursor anions from the one-dimensional channels of a porous copper chlorophosphate (CuCIP) framework, for the activation of O_2 and base-free oxidation of alcohols.^[10] It was demonstrated that calcination of the as-synthesised materials in air could generate fractions of supported, active NP catalysts for the aerobic oxidations, with Pt/CuCIP showing the best activity and selectivity. The development of sustainable oxidation catalysts relies on a detailed understanding of the nature of the active sites at a molecular level, which requires a multidisciplinary design-application approach, drawing on strengths of materials chemistry and spectroscopic characterization. By gaining in-depth knowledge of the local structural environment of the active centres within catalytic nanostructures (through x-ray absorption spectroscopy), we expect that precise structure–property correlations can be established, with a view to adopting a more generalized approach for the predictive design of single-site heterogeneous catalysts in industrially significant, sustainable oxidation reactions.

Herein we evaluate the propensity of Pt/CuCIP catalysts toward the activation of O_2 and TBHP for the selective oxidation of benzyl alcohol to benzaldehyde under batch conditions. Through detailed kinetic studies, activation energies are calculated in order to compare the ability of the catalysts to activate both oxidants, with the selectivity profiles which were

[a] C. S. Hinde, A. M. Gill, Dr. R. Raja
University of Southampton
Southampton SO17 1BJ (United Kingdom)
E-mail: R.Raja@soton.ac.uk

[b] Dr. P. P. Wells
UK Catalysis Hub
Oxon OX11 0FA (United Kingdom)

[c] Dr. P. P. Wells
University College London
London WC1H 0AJ (United Kingdom)

[d] Prof. T. S. A. Hor
Institute of Materials Research and Engineering (IMRE)
Agency for Science, Technology & Research (A*STAR)
3 Research Link, Singapore 117602 (Singapore)

[e] Prof. T. S. A. Hor
Department of Chemistry
National University of Singapore
3 Science Drive 3, Singapore 117543 (Singapore)

Supporting information for this article is available on the WWW under <http://dx.doi.org/10.1002/cplu.201500195>.

Part of a Special Issue to celebrate Singapore's Golden Jubilee. To view the complete issue, visit: <http://dx.doi.org/10.1002/cplu.v80.8>.

critically evaluated to establish the merits of each process. In addition, the effect of the calcination temperature on the activation of the catalyst will be studied, to determine its influence on the catalytic properties, in order to facilitate structure–property relationships.

A kinetic study was performed for the aerobic oxidation of benzyl alcohol by analysis of the conversion rates at different reaction temperatures. The reaction profile of the Pt catalyst was zero-order with respect to the conversion of benzyl alcohol, showing little dependence of the substrate concentration on the rate of reaction (Figure SI-4). Furthermore, the kinetic data was used to construct an Arrhenius plot (Figure 1 a) to calculate the activation energy for this reaction at 72.4 kJ mol^{-1} . Interestingly, it was noted in our earlier work^[10] that different reaction rates and selectivity profiles were observed for equivalent Au and Pd/CuCIP catalysts. These changes in the observed rates could, however, be due to the differing extents of extrusion in each material which is now thought to be a consequence of the activation temperature employed.

Investigation into the kinetics of the TBHP oxidation of benzyl alcohol using the same calcined (500 °C, 2 h) Pt/CuCIP catalyst (Fig-

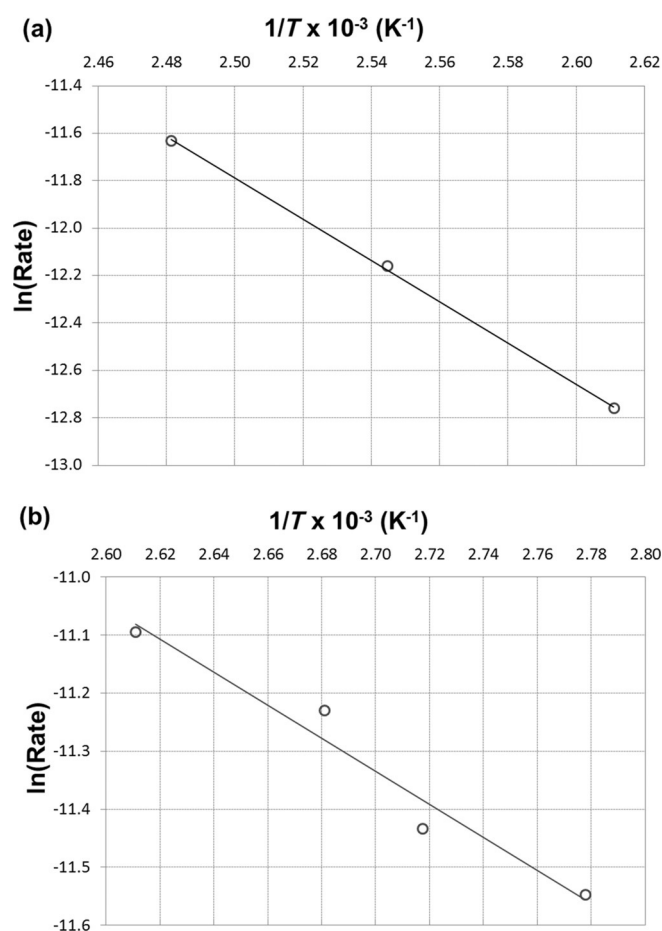


Figure 1. Arrhenius plots for the a) aerobic oxidation and b) TBHP oxidation of benzyl alcohol with the calcined (500 °C, 2 h) Pt/CuCIP catalyst. Conversion versus time plots and reaction conditions are given in Figure SI-1 (for a); Figure SI-2 (for b)).

ure 1b) revealed an activation energy of 23.6 kJ mol^{-1} under reaction conditions identical to those employed for the aerobic oxidation. This is also in agreement with the data obtained for analogous supported NP materials for peroxide oxidation of benzyl alcohol at $38^{[11]}$ and $20^{[12]}$ kJ mol^{-1} , whilst surpassing the values obtained for transition-metal catalysts based on Mo and W at 84 and 96 kJ mol^{-1} respectively.^[13] The lower activation energy of the peroxide-based oxidation is not surprising; given the lower BDE of TBHP relative to that of O_2 , and as reflected in the activity of the catalyst at temperatures lower than 100°C . With blank reactions not yielding appreciable conversions (Table SI-1), it is clear that the Pt/CuCIP catalyst is able to effectively activate both TBHP and O_2 as oxidants.

It is interesting to note the deviation from zero-order kinetics, as observed for the O_2 system, after low levels of conversion for the TBHP oxidation. The rate of benzyl alcohol oxidation with TBHP decreases over time and thus indicates a dependence on the concentration of the benzyl alcohol and/or TBHP in the reaction (Figure SI-5). In contrast, the selectivity of the TBHP oxidation is maintained at $>99\%$ throughout the course of the reaction, whereas benzoic acid is observed as a significant by-product in the aerobic oxidation (Figure SI-4). The higher temperature and pressure required for the O_2 oxidation could be responsible for the formation of the benzoic acid over-oxidation product.

For Pt NPs, it is generally accepted that the mechanism of action varies between aqueous and organic media,^[14] whereby water facilitates radical-type processes^[15] and organic media promotes heterolytic mechanisms, in analogy to reactions with Au NP systems. Through extensive studies on Au NPs, it has been determined that the adsorption of O_2 or peroxides can lead to activated surface-adsorbed superoxide or surface peroxide species that can facilitate the dehydrogenation process (Figure 2).^[16] The subsequent adsorption of the alcohol to form an adsorbed surface alcoholate species then occurs. Abstrac-

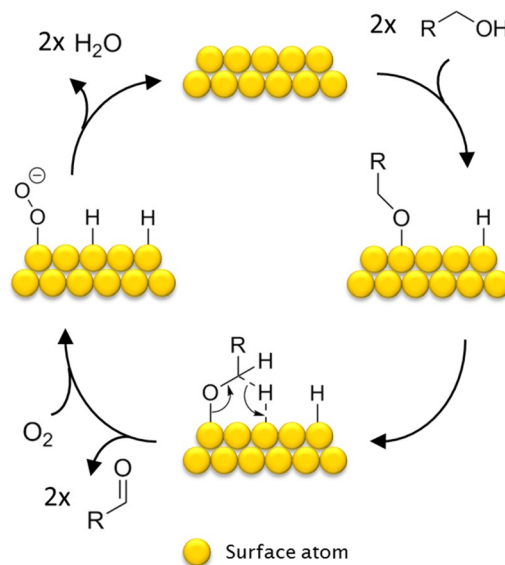


Figure 2. Mechanism for aerobic oxidation of an alcohol to an aldehyde on a metal NP surface in organic media.

tion of the β -hydride to the surface of the metal generates the desorbed aldehyde species, with the surface hydrides reacting with the activated surface peroxy species to form water and regenerate sites for adsorption and further catalytic cycles.^[17] It is likely that similar mechanisms operate also for Pt NP systems, including these Pt/CuClIP catalysts, in organic solvents.

Before we probed the catalytic properties of these materials an ideal candidate was to be selected and thus, a range of catalysts activated under different calcination temperatures (200–600 °C) were subjected to X-ray absorption fine structure (XAFS) analysis and compared in order to determine whether the extent of extrusion is indeed a function of temperature. The first-shell extended X-ray absorption fine structure (EXAFS) fitting parameters are shown in Table SI-2, along with the magnitude and imaginary components of the k^3 -weighted Fourier transform data and their corresponding fits in Figure SI-5. The EXAFS data shows a slight increase in Pt–Pt coordination numbers (0.8–1.2) and a respective decrease in Pt–Cl coordination (4.5–3.7), suggesting a minor correlation between the extent of NP formation and the calcination temperature. Despite the percentage errors, particularly with the lower coordination numbers being larger than desired, the trend is supported by comparisons in catalysis with TBHP. The conversions shown in Table 1 display a significant and progressive increase with catalyst calcination temperatures, which provide a clear indication that the activation temperature is directly related to NP formation (via extrusion), and that this has a direct influence on the catalytic activity of these materials.

Table 1. Conversions and product distributions from reactions conducted with Pt/CuClIP catalysts activated under increasing calcination temperature.^[a]

T [°C]	Conv. [%]	Benzaldehyde [%]	Benzoic acid [%]	Benzyl benzoate [%]
200	14.9	> 99.0	0.0	0.0
400	21.8	> 99.0	0.0	0.0
500	38.6	97.8	2.2	0.0
600	86.9	65.4	34.3	0.3

[a] Reaction conditions: 65 °C, 6 h, benzyl alcohol (27.7 mmol), substrate to oxidant (TBHP) mole ratio = 1.00:1.15, diethylene glycol dimethyl ether (11.2 mmol) and catalyst that had been calcined for 2 h (50 mg).

Nevertheless, it has been observed that when the calcination temperature exceeds 500 °C, the selectivity of the catalyst drastically diminishes. In addition, it was previously noted^[18] that these materials can undergo thermal degradation at temperatures above 600 °C, and indeed, inconsistencies in the powder X-ray diffraction patterns (PXRD) of these materials are observed at such elevated temperatures (Figure SI-6). Consequently, in all kinetic work reported herein the Pt/CuClIP catalysts were activated by calcination at 500 °C, and optimized oxidant to substrate ratios were used for maximizing the reaction selectivity towards benzaldehyde.

With the EXAFS fitting parameters presented in Table 2 taken into consideration, the Pt–Cl and Pt–Pt coordination

Table 2. EXAFS fitting parameters for the Pt/CuClIP material calcined for 2 h at 500 °C.^[a]

Abs Sc	N	R [Å]	2 σ^2 [Å ²]	E_f [eV]	R_{factor}
Pt–Cl	4.4(2)	2.320(6)	0.0026(4)	9(1)	0.013
Pt–Pt	1.4 (5)	2.78(2)	0.004(2)		

[a] Fitting parameters: $S_0^2 = 0.91$ as deduced by Pt foil standard; fit range $3 < k < 12.5$, $1 < R < 3$; number of independent points = 12. Abs Sc = Absorbing atom–Scattering atom.

numbers clearly show that only a fraction of the chlorometalate anions have been extruded to form metallic NPs on the surface of the materials, which is consistent with our earlier microscopy studies.^[10] As the rate of reaction is correlated with available active sites on the NP surface and the activation energy directly associated with the rates of reaction, it is noteworthy that the activation energies observed in our (partially) activated catalysts compete with those reported in the literature with analogous materials.^[11,12] Therefore, with an established method for complete extrusion, it should be possible to significantly improve on these values. Further analysis of activation parameters on structural properties and extent of extrusion is currently in progress.

In summary, a combination of spectroscopic and catalytic approaches have revealed that activation conditions play a crucial role in controlling the morphology, size and local structural environment of Pt nanoparticle catalysts, which are generated by a one-step extrusion process. Spectroscopic and kinetic analysis further illustrates that the presence of well-defined and isolated nanoparticles is fundamental to activating molecular oxygen for the aerobic oxidation of benzylic alcohols, and the ensuing structure–property correlations pave the way for the predictive design of solid catalysts. Comparison of activation energies showed a higher value for aerobic oxidation at 72.4 kJ mol^{−1}, compared with 23.6 kJ mol^{−1} for the TBHP oxidation. The aerobic oxidation sustained high rates of conversion with zero-order kinetics and thus negligible influence of substrate concentrations on reaction rates. On the other hand, the reaction had a reduced selectivity, with benzoic acid formed as a significant by-product, due to the high temperature and pressures required. Oxidation with TBHP maintained a high level of selectivity with negligible quantities of by-products formed. This was, however, limited by substrate concentration effects that resulted in considerably lower reaction rates after 4–5 h. The Pt/CuClIP NP catalyst was successful in activating both of these green alternative oxidants, bestowing unique advantages to each process, thereby affording considerable scope for the further exploitation of these catalysts and design strategy. Given the above, the oxidant can be opportunistically selected depending on whether selectivity for the aldehyde or acid is required, notwithstanding the requirement to maintain high reaction rates.

This general approach in evaluating oxidation potentials of nanoparticle-based materials, through the integration of detailed structural characterization and analysis of chemical environments, allows for precise molecular engineering of hetero-

geneous single-site nanocatalysts with applications in a wide array of organic processes. As hybrid nanomaterials have also been utilized elsewhere in hydrogenation and C–C coupling reactions,^[19] as well as for sensors,^[20] therapeutic agents and other bio-related applications,^[21] it is possible to envisage similar approaches to gain a fundamental understanding of materials for the development of new technologies.

Acknowledgements

C.S.H. thanks the University of Southampton for a VC scholarship. We thank Diamond Light Source for access to beamline B18 (SP8071-6) that facilitated and contributed to the results presented here. The UK Catalysis Hub is kindly thanked for resources and support provided via our membership in the UK Catalysis Hub Consortium and funded by EPSRC (portfolio grants EP/K014706/1, EP/K014668/1, EP/K014854/1 and EP/K014714/1). Support from NUS, IMRE & GSK is also gratefully acknowledged (grant no. R143-000-492-592).

Keywords: EXAFS · molecular oxygen activation · peroxide oxidation · platinum nanoparticles · selective oxidation

- [1] K.-G. Fahlbusch, F.-J. Hammerschmidt, J. Panten, W. Pickenhagen, D. Schatkowski, K. Bauer, D. Garbe, H. Surburg, *Ullmann's Encyclopedia of Industrial Chemistry*, Vol. 15, 7th ed., Wiley-VCH, Weinheim, **2003**, pp. 73–198.
- [2] a) F. Brühne, E. Wright, *Ullmann's Encyclopedia of Industrial Chemistry*, Vol. 5, 7th ed., Wiley-VCH, Weinheim, **2011**, pp. 223–235; b) J. L. Opgande, E. Brown, M. Hesser, J. Andrews, *Kirk-Othmer Encyclopedia of Chemical Technology*, John Wiley & Sons, New York, **2003**.
- [3] a) G. Franz, R. A. Sheldon, *Ullmann's Encyclopedia of Industrial Chemistry*, Vol. 25, 7th ed., Wiley-VCH, Weinheim, **2000**, pp. 543–600; b) I. W. C. E. Arends, R. A. Sheldon in *Modern Oxidation Methods* (Ed.: J.-E. Bäckvall), Wiley-VCH, Weinheim, **2004**, pp. 83–118.
- [4] R. A. Sheldon, *Chem. Soc. Rev.* **2012**, *41*, 1437–1451.
- [5] E. P. Clifford, P. G. Wenthold, R. Gareyev, W. C. Lineberger, C. H. DePuy, V. M. Bierbaum, G. B. Ellison, *J. Chem. Phys.* **1998**, *109*, 10293–10310.
- [6] V. I. Vedeneyev, *Bond Energies, Ionization Potentials and Electron Affinities*, Hodder & Stoughton Educational, London, **1966**.
- [7] a) Y.-F. Huang, M. Zhang, L.-B. Zhao, J.-M. Feng, D.-Y. Wu, B. Ren, Z.-Q. Tian, *Angew. Chem. Int. Ed.* **2014**, *53*, 2353–2357; *Angew. Chem.* **2014**, *126*, 2385–2389; b) J. Gong, C. B. Mullins, *Acc. Chem. Res.* **2009**, *42*, 1063–1073; c) D. Widmann, R. J. Behm, *Acc. Chem. Res.* **2014**, *47*, 740–749; d) D. I. Enache, J. K. Edwards, P. Landon, B. Solsona-Espriu, A. F. Carley, A. A. Herzing, M. Watanabe, C. J. Kiely, D. W. Knight, G. J. Hutchings, *Science* **2006**, *311*, 362–365.
- [8] a) A. Quintanilla, S. García-Rodríguez, C. M. Domínguez, S. Blasco, J. A. Casas, J. J. Rodríguez, *Appl. Catal. B* **2012**, *111–112*, 81–89; b) J. Ni, W.-J. Yu, L. He, H. Sun, Y. Cao, H.-Y. He, K.-N. Fan, *Green Chem.* **2009**, *11*, 756–759; c) V. Peneau, Q. He, G. Shaw, S. A. Kondrat, T. E. Davies, P. Miedziak, M. Forde, N. Dimitratos, C. J. Kiely, G. J. Hutchings, *Phys. Chem. Chem. Phys.* **2013**, *15*, 10636–10644.
- [9] a) Y. T. Lai, T. C. Chen, Y. K. Lan, B. S. Chen, J. H. You, C. M. Yang, N. C. Lai, J. H. Wu, C. S. Chen, *ACS Catal.* **2014**, *4*, 3824–3836; b) L. Kesavan, R. Tiruvalam, M. H. A. Rahim, M. I. bin Saiman, D. I. Enache, R. L. Jenkins, N. Dimitratos, J. A. Lopez-Sanchez, S. H. Taylor, D. W. Knight, C. J. Kiely, G. J. Hutchings, *Science* **2011**, *331*, 195–199; c) M. I. bin Saiman, G. L. Brett, R. Tiruvalam, M. M. Forde, K. Sharples, A. Thetford, R. L. Jenkins, N. Dimitratos, J. A. Lopez-Sanchez, D. M. Murphy, D. Bethell, D. J. Willock, S. H. Taylor, D. W. Knight, C. J. Kiely, G. J. Hutchings, *Angew. Chem. Int. Ed.* **2012**, *51*, 5981–5985; *Angew. Chem.* **2012**, *124*, 6083–6087; d) S. Ghosh, S. S. Acharyya, D. Tripathi, R. Bal, *J. Mater. Chem. A* **2014**, *2*, 15726–15733.
- [10] C. S. Hinde, S. Van Aswegen, G. Collins, J. D. Holmes, T. S. A. Hor, R. Raja, *Dalton Trans.* **2013**, *42*, 12600–12605.
- [11] G. Zhan, Y. Hong, F. Lu, A.-R. Ibrahim, M. Du, D. Sun, J. Huang, Q. Li, J. Li, *J. Mol. Catal. A: Chem.* **2013**, *366*, 215–221.
- [12] A. Mehri, H. Kochkar, G. Berhault, D. F. Cómbita Merchán, T. Blasco, *Mater. Chem. Phys.* **2015**, *149–150*, 59–68.
- [13] M. P. Chaudhari, S. B. Sawant, *Chem. Eng. J.* **2005**, *106*, 111–118.
- [14] N. Dimitratos, A. Villa, D. Wang, F. Porta, D. Su, L. Prati, *J. Catal.* **2006**, *244*, 113–121.
- [15] a) Y. Hong, X. Yan, X. Liao, R. Li, S. Xu, L. Xiao, J. Fan, *Chem. Commun.* **2014**, *50*, 9679–9682; b) T. Wang, H. Shou, Y. Kou, H. Liu, *Green Chem.* **2009**, *11*, 562–568.
- [16] A. Abad, A. Corma, H. García, *Chem. Eur. J.* **2008**, *14*, 212–222.
- [17] a) H. Tsunoyama, H. Sakurai, Y. Negishi, T. Tsukuda, *J. Am. Chem. Soc.* **2005**, *127*, 9374–9375; b) P. Frisrup, L. Johansen, C. Christensen, *Catal. Lett.* **2008**, *120*, 184–190.
- [18] E. R. Williams, R. M. Leithall, R. Raja, M. T. Weller, *Chem. Commun.* **2013**, *49*, 249–251.
- [19] a) G. Collins, M. Schmidt, C. O'Dwyer, J. D. Holmes, G. P. McGlacken, *Angew. Chem. Int. Ed.* **2014**, *53*, 4142–4145; *Angew. Chem.* **2014**, *126*, 4226–4229; b) Z. Wang, K.-D. Kim, C. Zhou, M. Chen, N. Maeda, Z. Liu, J. Shi, A. Baiker, M. Hunger, J. Huang, *Catal. Sci. Technol.* **2015**, *5*, 2788–2797.
- [20] J. Xie, Y. Zheng, J. Y. Ying, *Chem. Commun.* **2010**, *46*, 961–963.
- [21] B. H. Kim, M. J. Hackett, J. Park, T. Hyeon, *Chem. Mater.* **2014**, *26*, 59–71.

Received: April 29, 2015

Revised: June 12, 2015

Published online on June 29, 2015